J. Electrochem. Sci. Eng. **13(2)** (2023) 231-250; http://dx.doi.org/10.5599/jese.1343

Open Access : : ISSN 1847-9286
www.jESE-online.orghttp://www.jese-online.org/

Original scientific paper

Non-toxic leguminous plant leaf extract as an effective corrosion inhibitor of UNS S30403 in 1 M HCl

Okiemute Dickson Ofuyekpone[1,✉], Adeolu Adesoji Adediran[2,3,✉], Ochuko Goodluck Utu[4], Basil O. Onyekpe[5] and Ufuoma G. Unueroh[5]

[1]*Department of Metallurgical Engineering, Delta State Polytechnic, Ogwashi-Uku, Delta State, Nigeria*
[2]*Department of Mechanical Engineering, Landmark University, Omu-Aran, Kwara State, Nigeria*
[3]*Department of Mechanical Engineering Science, University of Johannesburg, South Africa*
[4]*Department of Welding and Fabrication, Delta State Polytechnic, Ogwashi-Uku, Delta State, Nigeria*
[5]*Department of Mechanical Engineering, University of Benin, Benin City, Edo State, Nigeria*

Corresponding authorc: ✉*okedickbest@yahoo.com*; ✉*dladesoji@gmail.com*, *Tel.: +234-803-411-9210*

Received: April 11, 2022; Accepted: September 23, 2022; Published: October 19, 2022

Abstract

Weight loss, polarization, and open circuit potential methods were used to investigate the corrosion inhibitory impact of Centrosema pubescens leaf extract on 304L austenitic stainless steel UNS S30403 in 1 M hydrochloric acid. This non-toxic extract behaves as a mixed-type inhibitor according to the polarization curves, thermodynamics and activation parameters. Both the weight loss calculations and potentiodynamic polarization investigations showed that 1.2 g L^{-1} was the optimal concentration of the leaf extract. While the weight loss method gave inhibition efficiency of 86.84 and 75.00 % after 10 and 60 days of immersion at the optimum concentration, polarization studies revealed inhibition efficiencies of 93.08 and 98.66 % at 303 and 333 K, respectively. The extract molecules adhered to the UNS S30403 surface according to Langmuir adsorption isotherm. The presence of the protective film on the UNS S30403 surface was confirmed by SEM, EDX, and XRD measurements. The inhibition performance of the leaf extract was noted to be a function of the extract concentration, immersion time and temperature. The FTIR analysis indicated an interaction between austenitic stainless steel UNS S30403 and the molecules of Centrosema pubescens leaf extract.

Keywords

Stainless steel 304L; green inhibitor; inhibition efficiency; protective film

Introduction

UNS S30403 austenitic stainless steel (304L) has a wide range of applications in a variety of industries. Usually, this type of stainless steel is protected by a highly protective film of chromium

oxyhydroxides and possesses excellent corrosion resistance in a wide range of aggressive environments. However, the UNS S30403 is easily attacked in acid solutions commonly used in industrial processes such as acid pickling, cooling systems, chemical and electrochemical etching, and oil well acidization.

It is worth noting that corrosion never stops, but its extent and severity can be reduced to a safe level. Corrosion control is a fundamental issue from an application standpoint, and it has been established that inhibitors, which act as barriers to lessen corrosion pitting assaults, are potent and should be employed [1-3]. Corrosion inhibitors have recently gained popularity as anticorrosion methods for stainless steel protection due to their ease of use, low cost, and high efficiency. Corrosion inhibitors are chemical substances added in small amounts to a corrosive environment. Most inhibitors contain noxious and lethal compounds, resulting in a ban on their use due to negative effects on the environment and humans. The safety and environmental issues raised by corrosion inhibitors of inorganic origin in industries have always been a worldwide concern [4,5].

In the past few decades, scientists have focused on the development of organic and environmentally friendly inhibitors. Nitrogen, sulfur, oxygen, and p-orbitals are present in the majority of organic compounds. These polar group structures can act as active centers, which are important in the adsorption of inhibitors onto the metal surface [6]. There have been numerous reports on the use of plant extracts as green metal inhibitors in acid solutions [7-12]. Watermelon rind, seed, and peel [7], *Curcuma longa* extract [8], *Aloe Vera* leaf extract [9], *Cucumis sativus* peel extract [10], *Salvia hispanica* [11], *Glycyrrhiza glabra* leaf extract [12], *Stylosanthes gracilis* leaf extract [13-15] and *Centrosema pubescens* leaf extract [16] were investigated for their inhibition properties. Nonetheless, more research on other plants that can be used as corrosion inhibitors in industrial applications is required. Also, it is necessary to evaluate the inhibitive capacity of the aforementioned plant extracts in several corrosive environments.

Centrosema pubescens is a member of the Fabaceae family, subfamily Faboideae, and tribe Phaseolae. It is also known as centro or butterfly pea and is a leguminous plant that can root at the nodes of trailing stems [16].

The goal of this study is to use various surface and electrochemical techniques to investigate the corrosion behavior of UNS S30403 in 1 M HCl in the presence of *Centrosema pubescens* leaf extract. The surface morphology of UNS S30403 specimens was also investigated.

Experimental

Preparation of UNS S30403 specimens

Specimens of austenitic stainless steel UNS S30403 with a composition of: 18.37 wt.% Cr, 8.01 wt.% Ni, 1.00 Mn, 0.39 wt.% Si, 0.03 wt.% C, 0.003 wt.% S, 0.04 wt.% P and the remainder is Fe, of dimensions 1×1×0.1 cm were used for various analyses. Before each analysis, two surface ends of each specimen were abraded with emery papers 220, 320, 550, 800, 1000 and 1200 grits. For the electrochemical study, 1 cm^2 surface area of the UNS S30403 was exposed to the 1.0 M HCl solution, while the remaining piece of the electrode was secured by epoxy resin.

Leaf extract and electrolyte preparation

Only matured leaves of *Centrosema pubescens* were collected, cleaned with water, and shade-dried for seventeen days. After that, dried leaves were pulverized and soaked in acetone for 72 h. Thereafter, the solution was filtered, and the filtrate was evaporated to remove the solvent from

the sample *via* a water bath. The prepared extract was then stored at 273 K in an airtight bottle until further use.

The leaf extract was used to prepare different concentrations of the extract solution by dissolving different amounts of the extract into the aggressive solution of interest. The active ingredients in *Centrosema pubescens* leaf extract were identified using gas chromatography/mass spectroscopy (GC/MS). The obtained results are presented in Table 1. The electrolyte solution of 1.0 M HCl was made by diluting 36 percent analytical grade hydrochloric acid with double distilled water. For weight loss and electrochemical studies, the inhibitor concentrations were kept between 0.2 and 1.4 g L^{-1}.

Table 1. *Active phytochemical ingredients found in the leaf extract of Centrosema pubescens by GC/MS characterization (using acetone as solvent)*

Name of phytochemical compound	Concentration, %	Molecular formula	Molecular weight, g mol^{-1}
2-Hexanol, 2-methyl-	6.74	$C_7H_{16}O$	116.2013
2-Butanamine, (S)-	1.41	$C_4H_{11}N$	73.1368
Oxirane, 2,2'-(1,4-butanediyl)bis-	20.66	$C_8H_{14}O_2$	142.195
11-(2-Cyclopenten-1-yl) undecanoic acid, (+)-	29.70	$C_{16}H_{28}O_2$	252.398
1,2:4,5:9,10-Triepoxydecane	2.91	$C_{10}H_{16}O_3$	184.235
1-Hexene, 6-bromo-	0.95	$C_6H_{11}Br$	163.056
Ethane,1,2-dicyclopropyl-	1.65	C_8H_{14}	110.1968
1,6-Hexanediol	1.67	$C_6H_{14}O_2$	118.17
Acetamide, N-2-propynyl-	0.90	C_5H_7NO	97.12
8-Nonynoic acid	6.94	$C_9H_{14}O_2$	154.209
7-Oxabicyclo[4.1.0]heptane, 3-oxiranyl-	10.48	$C_9H_{16}O_2$	156.2221
1-Cyclohexyl-1-propyne	1.14	C_9H_{14}	122.2075
1,10-Dichlorodecane	0.98	$C_{10}H_{20}Cl_2$	211.172
3-Octen-1-ol, (Z)-	0.81	$C_8H_{16}O$	128.2120
Methyl-4,6-ethylidene-alpha-d-galactopyranoside	2.93	$C_9H_{16}O_6$	220.221
Melezitose	4.91	$C_{18}H_{32}O_{16}$	504.4
1,3-Bis-(2-cyclopropyl,2-methylcyclopropyl)-but-2-en-1-one	0.80	$C_{18}H_{26}O$	258.4
4a,5,6,7,8,8a,10,10a-Octahydro-2H-1-oxa-9a-azaanthracen-9-one	1.61	$C_{12}H_{17}NO_2$	207.269
Cyclohept-4-enecarboxylic acid	1.02	$C_8H_{12}O_2$	140.18
Sucrose	1.14	$C_{12}H_{22}O_{11}$	342.3
1H-3a,7-Methanoazulene, octahydro-1,4,9,9-tetramethyl-	1.52	$C_{15}H_{26}$	206.3669

Weight loss measurement

In this study, UNS S30403 test specimens were firstly weighted and then fully immersed in 100 ml of 0.1 M HCl containing different concentrations of the leaf extract for 60 days (1440 hours). At each 10 days-interval, a test specimen was taken out from the tested solution, washed with distilled water, rinsed with acetone, dried, and re-weighed to determine the weight loss. The following equations were used to calculate the corrosion rate (*CR*) and inhibition efficiency (*IE*) [13 -15]:

$$CR = \frac{87.6W}{DAt} \quad (1)$$

$$IE = \frac{CR_a - CR_p}{CR_a} 100 \quad (2)$$

where *W* is weight loss in mg, *D* is density in g cm^{-3}, *A* = area in cm^2, *t* = exposure time in hours, and CR_a and CR_p are corrosion rates in the absence and presence of the inhibitor, respectively.

Electrochemical measurements

Potentiodynamic polarization measurements were used to investigate the electrochemical behaviour of the UNS S30403 austenitic stainless-steel samples in uninhibited and inhibited solutions. Polarization experiments were performed with an Autolab potentiostat (VersaSTAT 4) electrochemical system connected to a computer *via* a USB interface and the Versa Studio electrochemistry software package. Polarization measurements were performed using a standard three-electrode Pyrex glass cell at temperatures of 30 and 60 °C, respectively. A platinum rod served as the counter electrode in each case, while Ag/AgCl (3.5M KCl) served as the reference electrode, with a Luggin probe placed close to the working electrode. All experiments were carried out in aerated stagnant solutions. A working electrode was completely immersed in the aggressive solution for one hour until a stable open circuit potential (OCP) value is obtained. The potentiodynamic polarization study was carried out using a linear sweep technique at the scan rate of 1 mV s^{-1}, within the potential range of -0.25 to 0.25 V with respect to OCP. Tafel plots of potential *versus* the log of current density were used to calculate the corrosion current density (j_{corr}) and corrosion potential (E_{corr}). The corrosion rate (*CR*), the degree of surface coverage (θ) and the inhibition efficiency (*IE*) were calculated by eqs. (3-6) [6]:

$$CR = 0.00328 j_{corr} Eq / D \quad (3)$$

where j_{corr} = current density in μA cm^{-2}, *D* = density in g cm^{-3}, *Eq* = equivalent weight of stainless steel.

The inhibition efficiency was evaluated from j_{corr} values using the equation (4):

$$IE = 1 - \frac{j_{corr1}}{j_{corr2}} 100 \quad (4)$$

where j_{corr1} and j_{corr2} are corrosion current densities in the absence and presence of inhibitor, respectively. In addition, the polarization resistance (R_p) values were obtained from the measured j_{corr} values by applying the relationship (5)[6]

$$R_p = \frac{B}{j_{corr}} \quad (5)$$

where *B* is defined by eq. (6):

$$B = \frac{b_c b_a}{2.303(b_c + b_a)} \quad (6)$$

where b_c and b_a represent cathodic and anodic Tafel slopes.

Scanning electron microscopy (SEM)

VEGA3 TESCAN model scanning electron microscope was used to examine the morphology of test samples before and after immersion in 1.0 M HCl with and without the inhibitor.

X-ray diffraction analysis

The raw data was obtained using a RIGAKU MINIFLEX 600 X-ray diffractometer with mono-chromatic Cu Kα radiation produced at *k* = 0.154443 nm, and the patterns of the phases/films on the metal surface were identified using PANalytical XPERT HighScore in the absence and presence of the optimum concentration of *Centrosema pubescens* leaf extract. The diffraction patterns were captured at room temperature of 25 °C in the angular range of 2θ = 2 to 90°, with a step size of 2θ = 0.020° and a scan step time of 1.0 s. In both cases, the crystalline phases formed on the UNS S30403 stainless steel surface were identified using the ICDD-PDF database.

FTIR spectral analysis

The FTIR spectra were recorded using an Agilent Technologies Cary 630 FTIR to evaluate the composition of the corrosion product generated on the UNS S30403 surface.

Results and discussion

Weight loss measurements

The corrosion penetration rate and inhibition efficiency of UNS S30403 stainless steel in 1.0 M HCl solution with and without the addition of *Centrosema pubescens* leaf extract, measured by weight loss in 10 day-intervals during 60 days of immersion, were calculated using eqns. (1) and (2), and listed in Table 2.

***Table 2**. Corrosion rates (CR) and inhibition efficiencies (IE) obtained by weight loss measurements in 10 day-intervals after exposing UNS S30403 specimens to 1.0 M HCl solution during 60 days without and with different concentrations of* Centrosema pubescens *leaf extract*

$c_{leaf\ extract}$ / g L^{-1}	10th day		20th day		30th day		40th day		50th day		60th day	
	CR / mm y^{-1}	*IE* / %	*CR* / mm y^{-1}	*IE* / %	*CR* / mm y^{-1}	*IE* / %	*CR* / mm y^{-1}	*IE* / %	*CR* / mm y^{-1}	*IE* / %	*CR* / mm y^{-1}	*IE* / %
Blank	1.76	--	1.23	--	1.10	--	1.10	--	0.99	--	0.93	--
0.2	1.07	39.47	0.84	32.08	0.82	25.35	0.87	20.21	0.83	16.82	0.80	14.17
0.4	0.93	47.37	0.63	49.06	0.63	42.25	0.67	38.30	0.67	32.71	0.63	31.67
0.6	0.70	60.53	0.46	62.26	0.50	54.93	0.53	51.06	0.52	47.66	0.63	44.17
0.8	0.56	68.42	0.39	67.92	0.37	66.20	0.37	65.96	0.34	65.42	0.47	55.00
1.0	0.42	76.32	0.30	75.47	0.31	71.83	0.30	72.34	0.28	71.96	0.24	70.00
1.2	0.23	86.84	0.21	83.02	0.25	77.46	0.24	77.66	0.24	75.70	0.80	75.00
1.4	1.21	31.58	1.00	18.87	0.93	15.49	0.93	14.89	0.87	12.15	0.93	9.17

Results from Table 2 are better visualized by the 3-D graph presented in Figure 1, which depicts the variation of the corrosion rate of stainless steel in 1 M HCl solution caused by the change of leaf extract concentration, as well as immersion time. Obviously, the corrosion rate was reduced by the addition of the *Centrosema pubescens* leaf extract up to the concentration of 1.2 g L^{-1}. The decrease in corrosion rate is a consequence of the increase in extract concentration, which implies that more extract molecules were adsorbed on the metal surface, providing higher surface coverage and suppressing both the anodic and cathodic reaction [17].

Similarly, Figure 2 depicts the relationship between inhibition efficiency, the concentration of *Centrosema pubescens* leaf extract, and immersion time, revealing a strong influence of the leaf extract on the system. It can be seen that the inhibition efficiency was higher for a higher concentration of the leaf extract. This indicates that the compact barrier film was formed on the metal surface, effectively separating the surface from aggressive anionic species and stifling the redox reactions associated with the corrosion process. As shown in Figure 2, at all immersion times, the inhibition efficiency of the leaf extract increases with its concentration. The highest *IE* value of 86.84 % was reached after 10 days of immersion at the optimum leaf extract concentration of 1.2 g L^{-1}. The observed increase in inhibition efficiency with increasing extract concentration could be attributed to an increase in surface coverage caused by the adsorption of extract molecules onto the steel surface. This suggests that the corrosion inhibition performance of *Centrosema pubescens* leaf extract is largely due to its ability to provide a strong adherent and stable film on the metal surface. This film inhibits penetration of chloride ion reacting species which initiate and sustain corrosion reactions, as well as diffusion of Fe^{2+} ions from the electrode surface [18].

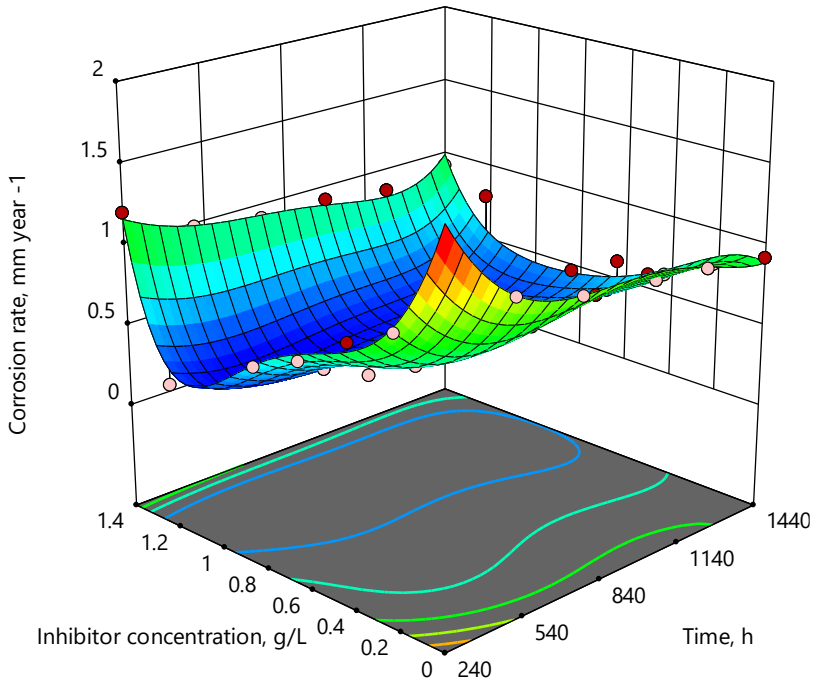

***Figure 1**. 3-D surface plot showing the interaction between corrosion rate, inhibitor concentration and immersion time for Centrosema pubescens leaf extract in 1.0 M HCl solution*

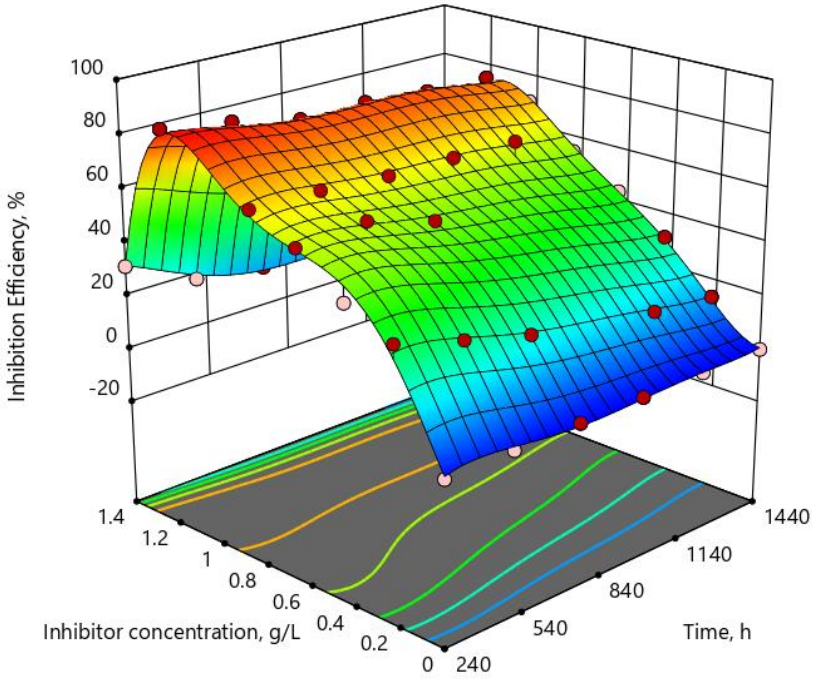

***Figure 2.** 3-D surface plot showing the interaction between inhibition efficiency, inhibitor concentration and immersion time for* Centrosema pubescens *leaf extract in 1.0 M HCl solution*

As also shown in Figures 1 and 2 and data in Table 2, the increase of the leaf extract concentration beyond 1.2 g L^{-1}resulted in a sudden increase in corrosion rate and a significant decrease in inhibition efficiency. This implies that the leaf extract becomes harmful when present at higher than optimal concentration, possibly due to the desorption of inhibitor at the metal–electrolyte interface [18]. On the other hand, the corrosion rate and the inhibition efficiency were found to have an inverse relationship with immersion time. The observed decrease in corrosion rate with immersion

time connotes that the reactivity of UNS S30403 in the specified acidic solution decreased over time, whereas a decrease in inhibition efficiency can be attributed to desorption [16].

Electrochemical measurements

Open circuit potential (OCP) versus leaf extract concentration

Plots of OCP values of the UNS S30403 electrode against the concentration of the leaf extract in 1.0 M HCl, measured after 600 s of immersion at two temperatures (303 and 333 K), are shown in Figure 3. The graph shows that adding *Centrosema pubescens* leaf extract shifts the OCP value in a positive direction. Generally, a shift of OCP value to more negative values indicates that metal is corroding, *i.e.,* any protective coating established on the metal surface is going to dissolve. If the OCP value is shifted to the noble direction (as is happening here), it would mean that the metal surface is protected by the formation of a corrosion products film. It has also been demonstrated that adsorption of the leaf extract is more favored at higher temperatures, as the positive shift in OCP is greater at higher temperatures [19,20].

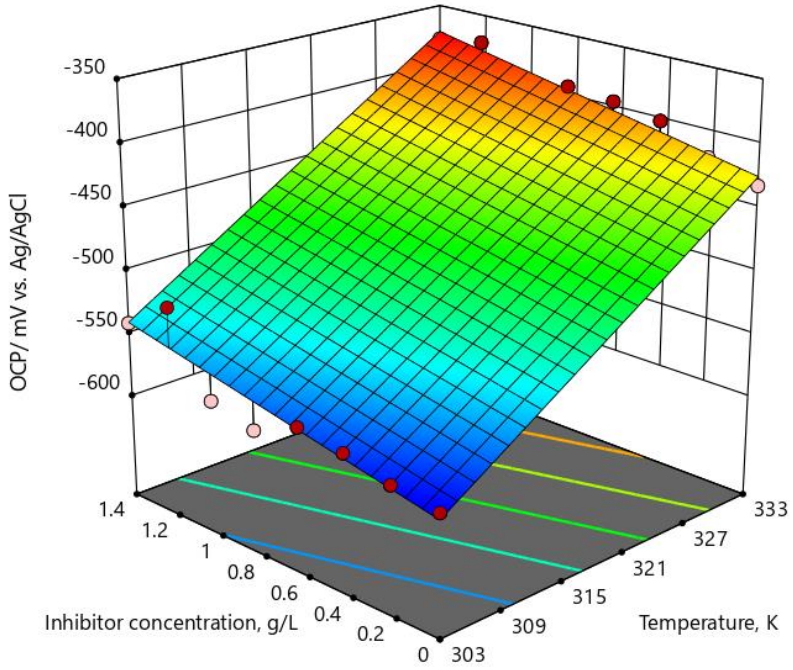

Figure 3 *OCP values of UNS S30403 specimens in 1 M HCl solution versus concentration of* Centrosema pubescens *leaf extract after 600 s of immersion at 303 and 333 K*

Tafel polarization measurements

Plots of Figure 4 depict the relationships between current density and potential for UNS S30403 in 1.0 M HCl with various concentrations of *Centrosema pubescens* leaf extract, measured at two temperatures. At both temperatures, Figures 4 (a) and (b) illustrate a positive shift of corrosion potential (E_{corr}) toward a more passive region after the addition of the leaf extract into the systems. This shift in E_{corr} in a positive direction suggests that increasing the concentration of the extract in the test media increases the corrosion resistance of the UNS S30403 [21]. Typically, the changes in polarization curves observed after the addition of the inhibitor are used to classify inhibitors as either cathodic, anodic, or mixed.

According to Figure 4, both anodic and cathodic polarizations are influenced concurrently and to almost the same extent, indicating that *Centrosema pubescens* leaf extract influences both anodic and cathodic reactions, *i.e.,* hydrogen evolution and metal dissolution.

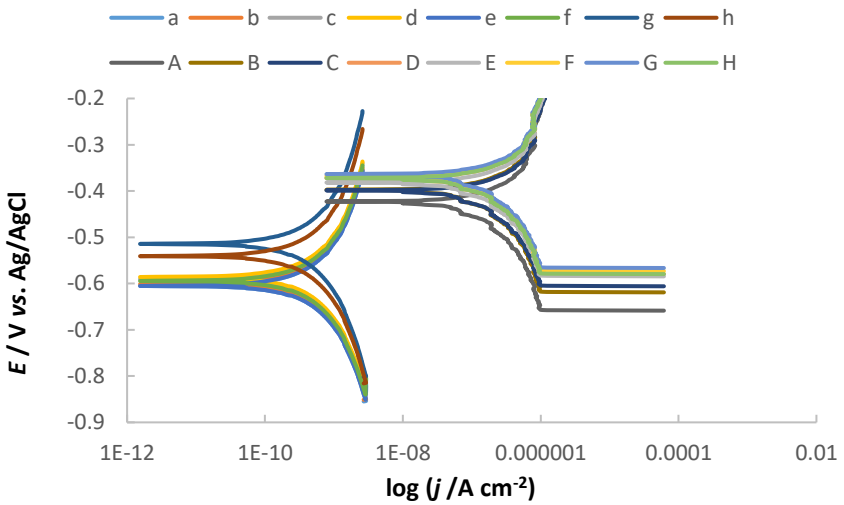

***Figure 4**. Polarization curves for UNS S30403 specimen corrosion in 1.0 M HCl solution without (a) and with different concentrations, 0.2-1.4 g L^{-1} (b – h) of* Centrosema pubescens *leaf extract at 30 °C, and without (A) and with different concentrations, 0.2-1.4 g L^{-1} (B – H) of* Centrosema pubescens *leaf extract at 60 °C*

Essentially, when the change in E_{corr} is greater than ±85 mV, an inhibitor is classified as either anodic or cathodic, while lower values indicate a mixed-type inhibitor [22]. Figure 4 shows that the greatest change of E_{corr} in the presence of the applied leaf extract is 72 mV at 30 °C and 59 mV at 60 °C, respectively. This suggests that the *Centrosema pubescens* leaf extract acts as a mixed-type inhibitor [23,24].

Values of corrosion parameters derived from potentiodynamic polarization curves in Figure 4, *i.e.,* corrosion potential, corrosion current density, cathodic and anodic Tafel at two temperatures (303 and 333 K), are listed in Table 3. In addition, Table 3 lists the parameter values calculated by eqs. (3-6), *i.e.,* corrosion rate, inhibition efficiency, polarization resistance, and surface coverage fraction. The fractional surface coverage by extract molecules (θ) was computed by dividing the inhibition efficiency defined by eq. (4) by 100.

***Table 3.** Parameters of potentiodynamic polarization curves obtained during corrosion of alloy 304L in 1.0 M HCl containing diverse concentrations of Centrosema pubescens leaf extract*

Temperature	$c_{inhibitor}$ / g L^{-1}	E_{corr} / mV	b_c / mV dec^{-1}	b_a / mV dec^{-1}	j_{corr} / mA cm^{-2}	R_p / Ω cm^2	CR / mm $year^{-1}$	IE / %	θ
303 K	0	-588	49	63	0.0405	296	0.470	--	--
	0.2	-583	65	62	0.0108	1281	0.125	73.42	0.7342
	0.4	-574	57	60	0.0089	1426	0.103	78.01	0.7801
	0.6	-569	58	56	0.0074	1667	0.086	81.67	0.8167
	0.8	-586	53	50	0.0058	1913	0.068	85.57	0.8557
	1	-577	60	57	0.0043	2980	0.049	89.48	0.8948
	1.2	-516	61	59	0.0028	4651	0.033	93.08	0.9308
	1.4	-541	60	495	0.0179	1300	0.208	55.73	0.5573
333 K	0	-432	121	43	0.4394	31	5.100	--	--
	0.2	-420	120	55	0.091	180	1.056	79.29	0.7929
	0.4	-401	90	56	0.0564	266	0.655	87.16	0.8716
	0.6	-395	84	77	0.0299	583	0.347	93.20	0.9320
	0.8	-392	82	80	0.0151	1164	0.175	96.56	0.9656
	1	-396	44	91	0.0101	1271	0.118	97.69	0.9769
	1.2	-373	45	97	0.0059	2274	0.068	98.66	0.9866
	1.4	-378	47	100	0.1449	96	1.682	67.02	0.6702

According to data in Table 3, at both temperatures (303 and 333 K), inhibition efficiency, degree of surface coverage, and polarization resistance values increased with an increase of leaf extract concentration up to the concentration of 1.2 g L^{-1}. At the same time, the corrosion current density and corrosion rate varied inversely with leaf extract concentration, showing the lowest values at 1.2 g L^{-1}. At each leaf extract concentration, as well as for blank solution, corrosion currents and corrosion rates are significantly lower at a lower temperature (303 K) than at a higher temperature (333 K), while the opposite is true for *IE*, θ and R_p values. Thus, for the extract concentration of 1.2 g L^{-1}, corrosion current density reached its lowest value of 0.0028 mA cm^{-2} at 30 °C and 0.00587 mA cm^{-2} at 60 °C, respectively. At the same time, the polarization resistance value increased considerably, from 296 (blank) to 4651 Ω cm^2 at 1.2 g L^{-1} of leaf extract at 30 °C and from 31 (blank) to 2274 Ω cm^2 at 1.2 g L^{-1} of leaf extract at 60 °C. These changes of j_{corr} and R_p values can be connected with extract molecules that react with liberated iron (Fe^{2+}) ions to generate a layer of corrosion products, which forms a barrier between the metal and the environment. This barrier makes metal contact with corrosive solution ions more difficult, lowering thus the corrosion current density and increasing R_p values. However, data in Table 3 show that corrosion current density and corrosion rate increased at the leaf extract concentration higher than 2 g L^{-1}. This can be explained by the inhibitor molecules with the same electric charge, and at high adsorbed quantities, they repel each other electrostatically. This causes the extract components to desorb from the UNS S30403 surface, leaving the metal at desorption sites fully exposed to the corrosive solution. Also, data in Table 3 show that increasing the extract concentration up to 1.2 g L^{-1} increases its inhibition efficiency value, while higher concentrations reduce it. The fractional surface coverage by extract molecules behaves similarly to the extract inhibition efficiency. With the addition of 1.2 g L^{-1}, the greatest *IE* values of 93.08 and 98.66 % were obtained at 30 and 60 °C, respectively. This significant improvement in the extract inhibition efficiency at a higher temperature, also shown in Figure 5, suggests that more of the extract was strongly adsorbed at a higher temperature.

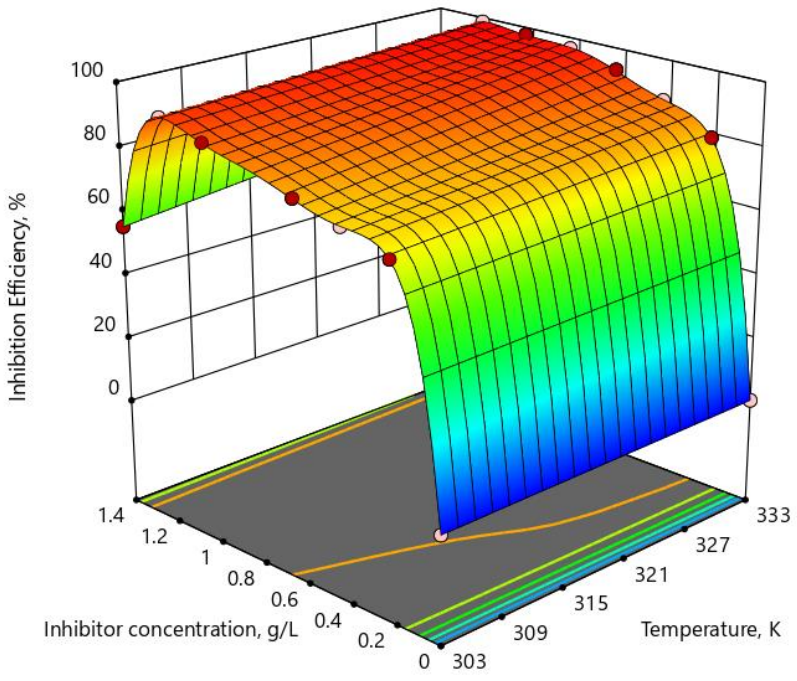

Figure 5. *Inhibition efficiency vs. concentration of* Centrosema pubescens *leaf extract for UNS S30403 in 1.0 M HCl at 303 and 333 K, determined by potentiodynamic polarization*

Thus, the inverse relationship that exists between polarization resistance and registered corrosion current density suggests that protective films with improved properties (as the temperature was increased from 30 to 60°) were formed. These films act as a barrier at the metal-solution interface, reducing the anodic dissolution of the UNS S30403 and modifying and inhibiting the evolution of the H^+ ion discharge [25,26].

As a result, the current findings show that for a relatively low concentration of 1.2 g L^{-1} of *Centrosema pubescens* leaf extract, high inhibition efficiency is achieved and the corrosion current density value is substantially and significantly reduced.

Scanning electron microscopy (SEM)

Figures 6(a-c) show SEM micrographs of the UNS S30403 surface in the as-received state and after ten days (240 hours) of immersion in the absence and presence of the optimum concentration (1.2 g L^{-1}) of the *Centrosema pubescens* leaf extract in 1.0 M HCl.

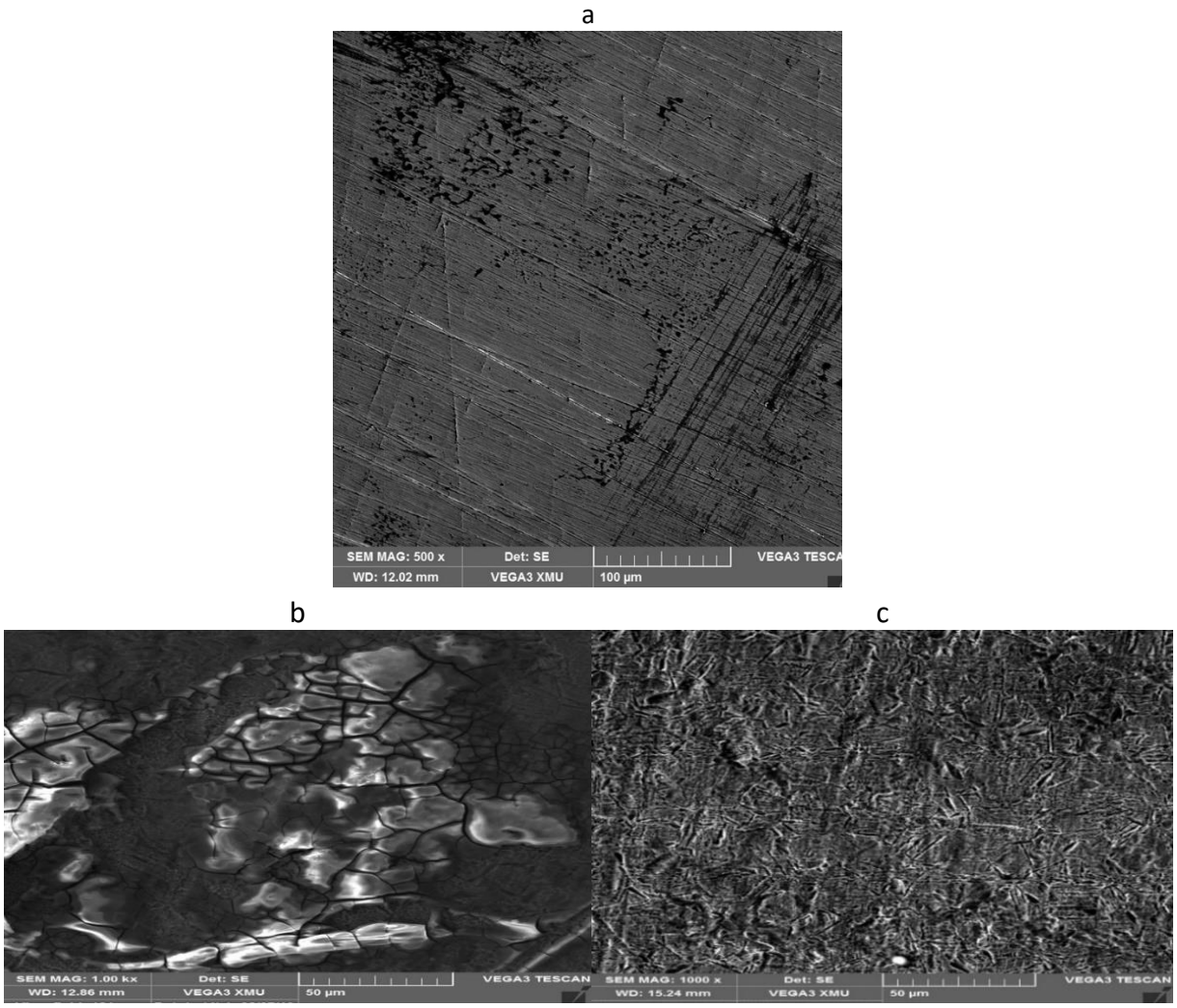

Figure 6. *SEM images of UNS S30403: as-received (a), and immersed for 240 h in 1.0M HCl in the absence (b), and presence (c) of the optimum leaf extract concentration (1.2 g L^{-1})*

It can be seen in Figure 6a that the polished UNS S30403 surface is smooth and free of pits but with obvious lines resulting from cutting during preparation. However, for the surface corroded for ten days in 1.0 M HCl without leaf extract, severe damage, with pits and cracks, appeared (Figure 6b). Normally, Figure 6b shows an extremely rough and porous surface that corroded in the absence of extract. A great number of pits, micro pits, and highly corroded topography of UNS S30403 stainless

steel coupons are visible as a result of corrosive effects of chloride ions, caused by the breakdown of the passive coating of chromium oxide. The rate of re-passivation of the steel is faster than the rate of diffusion of aggressive anions through cracks of the passive film. The adsorbed oxygen species and chromium cations responsible for passivation are displaced by chloride ions which diffuse from bulk solution into the oxide/liquid interface of the steel surface, whereas Fe^{2+} ions diffuse into the solution. This results in the quick creation of voids, which form and proliferate in specified locations such as defect and flaw regions, inclusions, and pitting-prone areas in general. When the UNS S30403 specimen surface is exposed to the optimum concentration of the *Centrosema pubescens* extract in the 1.0 M HCl acid solution (Figure 6c), a stable protective layer is formed on the steel surface, which acts as a barrier to charge and mass transfer. As seen in Figure 6c, this resulted in a sharp modification in the morphology of the UNS S30403 surface compared to Figure 6b and, consequently, improved properties on the surface of the stainless steel [27].

Energy dispersive X-ray analysis (EDX)

The compositional information of the surface of the UNS S30403 sample in 1.0 M HCl in the absence and presence of the *Centrosema pubescens* leaf extract was obtained using energy dispersive X-ray analysis. Figures 7(a) – (c) show EDX spectra obtained for the specimens in the as-received state and specimens left for 10 days in 0.1 M HCl in the absence and presence of the optimum concentration of the leaf extract.

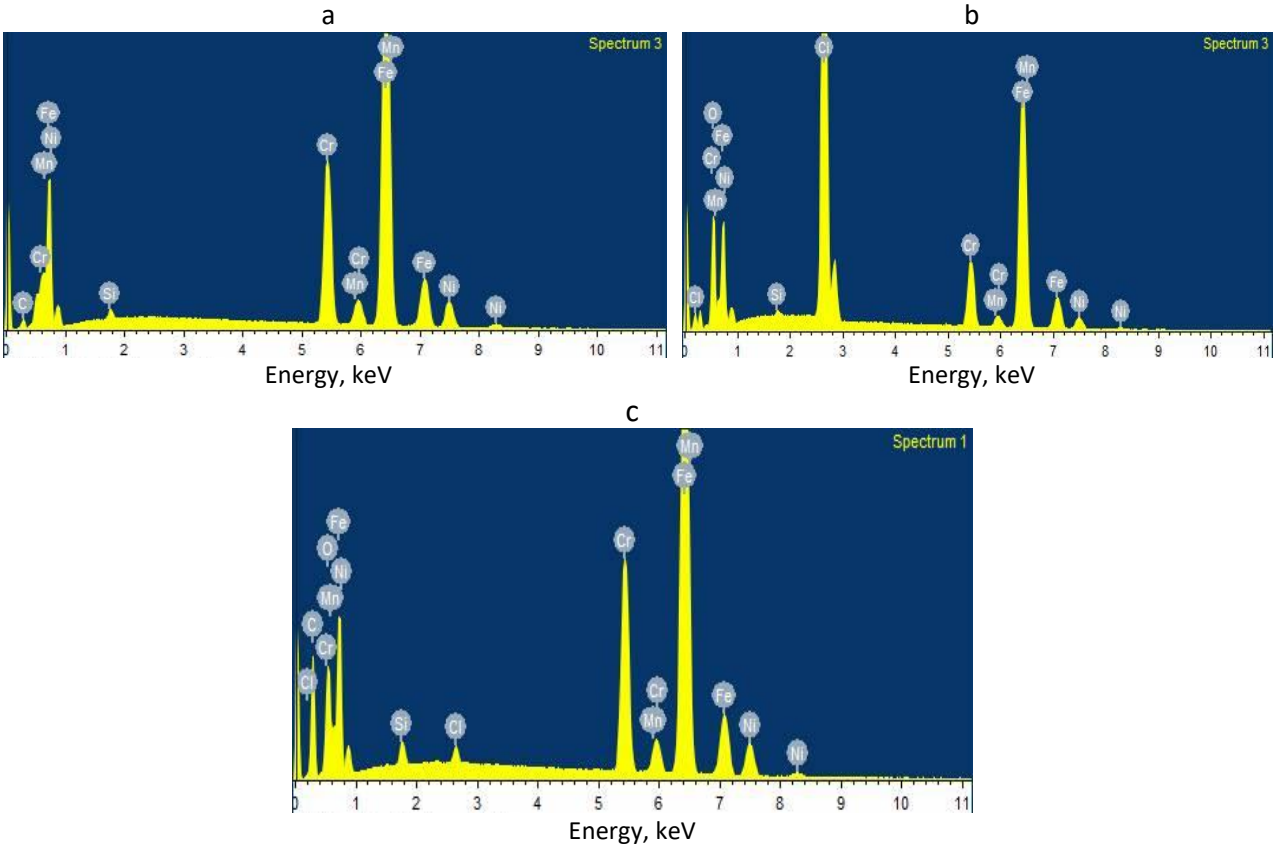

Figure 7. *EDX spectra of UNS S30403 surface: (a) as-received; after 10 days of immersion in (b) blank 1.0M HCl solution and (c) 1.0M HCl with 1.2 g L^{-1} Centrosema pubescens leaf extract*

High peaks of Fe, Mn, Cr, and Ni in the EDX spectrum of the as-received specimen shown in Figure 7a confirm that the adsorbent is stainless steel of 300 family. A conspicuous and visible presence of peaks of chloride ions can be seen in the EDX spectrum of Figure 7b, obtained after immersing the

UNS S30403 coupons in 1.0M HCl without adding the extract. The chloride ion peak was, however, noticeably reduced after the introduction of *Centrosema pubescens* leaf extract at the optimum concentration of 1.2 g L^{-1} (Figure 7c). This observation attests the inhibitory potential of the leaf extract in reducing the rate of corrosion in HCl solutions [27,28].

Adsorption isotherm

The adsorption of an extract at the metal/solution interface is thought to be related to its performance as a corrosion inhibitor in acidic solutions. To ensure the effective adsorption of an extract on a metal surface, the reciprocity force between metal and extract must be greater than the synergistic force between metal and water molecules [29]. As a result, the adsorption isotherm can be used to understand corrosion inhibition processes. Despite the existence of several adsorption isotherms, the magnitudes of the coefficient of determination values (correlation coefficients) were used as indices for selecting the Langmuir isotherm for the corrosion adsorption processes of *Centrosema pubescens* leaf extract on the UNS S30403 surface in 1.0 M HCl solution. The fit to the Langmuir isotherm was determined by plotting c/θ versus c according to eq. (7):

$$\frac{c}{\theta} = \frac{1}{K_{ads}} + c \qquad (7)$$

where K_{ads} is adsorption/desorption equilibrium constant (L g^{-1}), θ is surface coverage, and c is the concentration of inhibitor (g L^{-1}).

The Langmuir isotherm plots at 303 and 333 K are depicted in Figure 8, while the corresponding values of slope and intercept of straight lines are, together with calculated K_{ads}, shown in Table 4.

It is worth noting that the basic assumptions of the Langmuir adsorption isotherm [30] are as follows: I. The metal surface is homogeneous; II. the adsorbate is adsorbed specifically, with each adsorbed species occupying only one surface site; III. adsorbed compounds do not diffuse on the surface, and IV. the standard adsorption-free energy is unaffected by the degree of coverage.

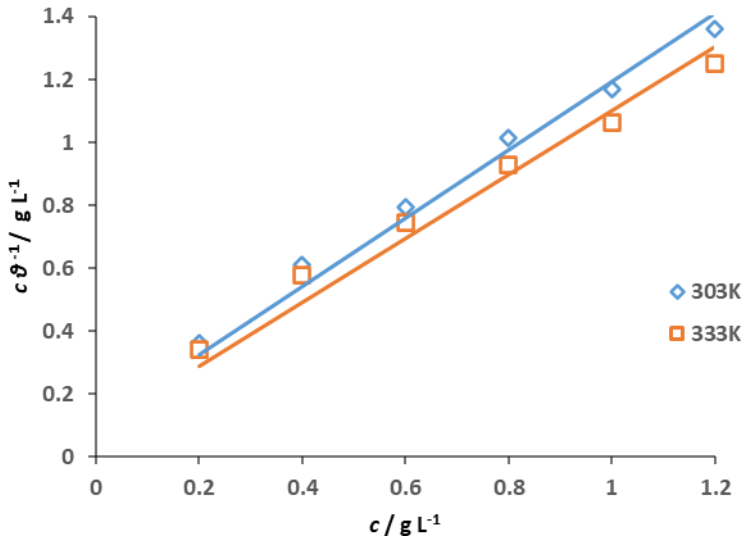

Figure 8. *Langmuir adsorption isotherms for Centrosema pubescens leaf extract (0.2– 1.2 g L^{-1}) on UNS S30403 stainless steel surface in 1.0 M HCl solution at 303 and 333 K*

Table 4*. Langmuir adsorption isotherm and thermodynamic parameters for adsorption of Centrosema pubescens leaf extract on UNS S30403 stainless steel surface in 1M HCl*

Temperature, K	Slope	Intercept	K_{ads} / L g^{-1}	R^2	ΔG^o_{ads} / kJ mol^{-1}
303	1.0141	0.1004	9.96	0.9959	-23.20
333	1.0139	0.018	55.56	0.9998	- 30.25

As seen in Table 4, straight lines with coefficients of determination R^2 = 0.9959 and 0.9998 at 303 K and 333 K, respectively, were obtained from the Langmuir isotherm equation, but the slopes are not exactly equal to unity. These slopes refute the Langmuir adsorption isotherm postulation of monolayer adsorption of inhibitor molecules on the adsorbent surface, despite R^2 values being acceptable for the Langmuir isotherm. This discrepancy could be due to the limitations inherent in using the Langmuir adsorption isotherm to fit data from typical metal inhibition processes; for example, monolayer inhibitor adsorption is only possible on homogeneous metal surfaces and without adsorbed molecules diffusion at any temperature [31]. Anyhow, it is impossible to fully accept these assumptions even for a typical acid inhibition system like the one under consideration because foreign ions and interactions in the same medium are possible. Also, some adsorption processes may be potential dependent and selective in terms of the types of charges on the metal surface. According to [31], another physical feature of the adsorption isotherm must be considered to explain these digressions as they affect the adsorption mechanism. As a result, the Langmuir adsorption isotherm can be mathematically modified to account for the dimensionless separation constant, K_L, as shown in equation (8).

$$K_L = \frac{1}{1 + K_{ads} c} \tag{8}$$

where K_L is the dimensionless separation factor of the extract adsorption, K_{ads} is the adsorption/desorption equilibrium constant and c = concentration of the extract.

The calculated values of K_L for various concentrations of *Centrosema pubescens* leaf extract at 303 and 333 K for UNS S30403 in 1 M HCl are shown in Table 5.

Table 5. *Values of dimensionless separation factor, K_L, for varied concentrations of Centrosema pubescens leaf extract at 303K and 333K for 304L stainless steel corrosion in 1 M HCl*

$c_{leaf\ extract}$ / g L^{-1}	K_L	
	303 K	333 K
0.2	0.334	0.083
0.4	0.201	0.043
0.6	0.143	0.029
0.8	0.112	0.022
1.0	0.091	0.018
1.2	0.077	0.015
1.4	0.067	0.012
Mean	0.146	0.032

In general, for values of K_L > 1, adsorption is unfavorable and inconsistent with the Langmuir adsorption isotherm). For K_L < 1, adsorption is favorable and experimental data fit the Langmuir adsorption isotherm), while K_L = 1 and K_L = 0 connote that the adsorption is linear and irreversible, respectively. Table 5 shows that all K_L values for all inhibitor concentrations are less than unity, indicating that the adsorption process is well aligned with the Langmuir isotherm. Furthermore, the inhibitive potency of *Centrosema pubescens* leaf extract is more favorable at higher temperatures, based on the estimated mean value of K_L for each temperature [31]. For the adsorption process, the adsorption/desorption equilibrium constant (K_{ads}) is related to the free energy of adsorption, ΔG^o_{ads}, through the eq. (9) [32]:

$$K_{ads} = \frac{1}{c_{solvent}} \exp \frac{-\Delta G^o_{ads}}{RT} \tag{9}$$

where R is molar gas constant (J mol^{-1}), T is the temperature (K), $c_{solvent}$ is the concentration of water in solution (g L^{-1}), K_{ads} is the adsorption/desorption equilibrium constant (L g^{-1}) obtained from the intercept of straight line in Figure 8, and ΔG^{o}_{ads} is free energy change of adsorption (kJ mol^{-1}). It is understandable that the unit of $c_{solvent}$ is a function of that of K_{ads}. As pointed out in Table 4, the unit of K_{ads} is L g^{-1}, and so the unit of C solvent is g L^{-1} with a value of approximately 10^3 [33].

The outcome of calculations displayed in Table 4 indicates that the values of ΔG^{0}_{ads} calculated by eq. (8) are negative, which clearly indicates spontaneous adsorption of the extract molecules. Higher K_{ads} value obtained at higher temperatures suggests that adsorption is more favored at higher temperatures [30,33]. Accordingly, the obtained values of ΔG^{0}_{ads} showed that a mixed mode of adsorption is occurring. This assertion is because the calculated values of ΔG^{0}_{ads} listed in Table 4 reveal values of -23.20 and -30.25 kJ mol^{-1} at 303 K and 333 K, respectively. Usually, ΔG^{0}_{ads} values of 20 kJ mol^{-1} or less are associated with electrostatic interaction between charged organic molecules and charged metal surface (physisorption), while those of 40 kJ mol^{-1} or higher are associated with charge sharing or transfer from the organic molecules to the metal surface to form a coordinate type of bond (chemisorption) [6,32]. The observed combined mode of adsorption (physisorption and chemisorption) could be attributed to the fact that *Centrosema pubescens* leaf extract contains a variety of chemical compounds (*cf*. Table 1), where depending on the temperature, some can be adsorbed chemically and others physically [34].

XRD analysis

Figure 9 shows X-ray diffraction (XRD) patterns of UNS S30403 stainless steel surfaces from both the extract-free and extract-present acid test solutions. For a better understanding of corrosion processes, phase compositions (as opposed to elemental compositions) must be described.

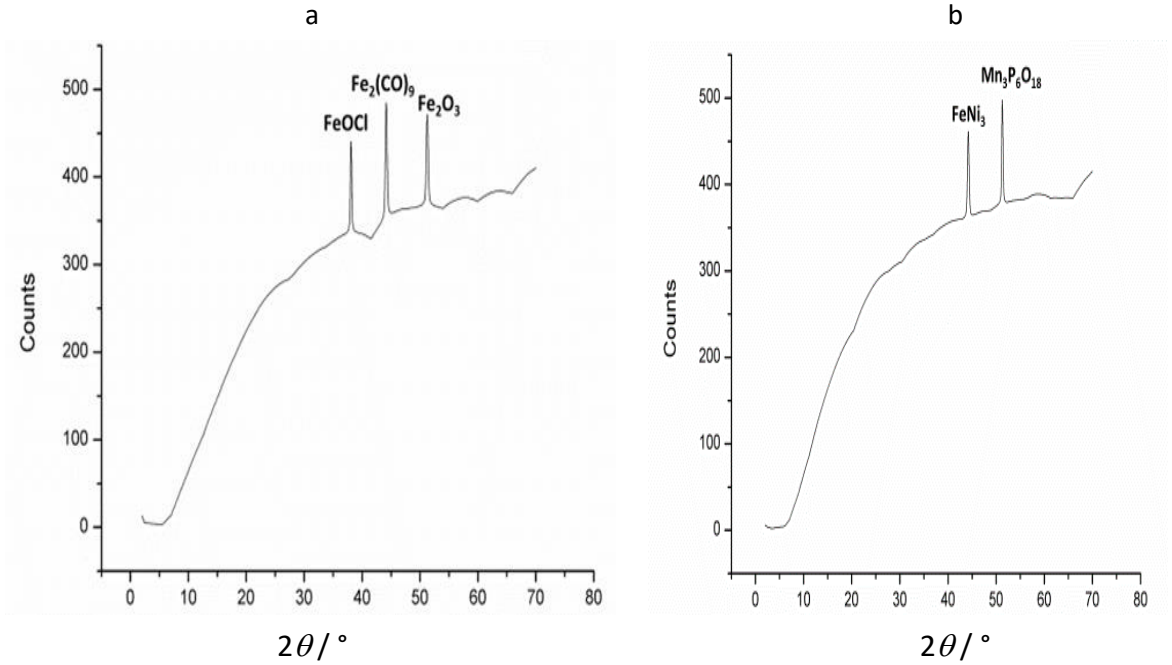

Figure 9. *XRD spectra showing phases formed on UNS S30403 surface in 1.0M HCl: a) blank solution; b) in the presence of 1.2 g L^{-1} Centrosema pubescens leaf extract*

Information on phase compositions is useful for both explaining the corrosion process and locating the source of corrosion in a facility while also providing solutions to the problem [35]. Figure 9a shows the presence of Fe_2O_3, $Fe_2(CO)_9$ and FeOCl, typical of a corroding system [36]. The addition

of the leaf extract of *Centrosema pubescens* to the corrosive system helped to drastically minimize the corrosive effect of chloride ions in the HCl solution, as the XRD patterns of the surface in Figure 9b showed no peak for Fe_2O_3, $Fe_2(CO)_9$ and FeOCl. This indicates that a protective film capable of stifling the corrosion reaction is developed on the surface of UNS S30403 stainless steel [36].

Thermodynamic and activation parameters

Influence of temperature on corrosion of UNS S30403 in 1.0 M HCl solution without and in the presence of various concentrations of the *Centrosema pubescens* leaf extract was investigated using the logarithmic form of Arrhenius equation (10) [20]:

$$\log\frac{CR_1}{CR_1} = \frac{E_a}{2.303R}\left(\frac{1}{T_1} - \frac{1}{T_2}\right) \quad (10)$$

where CR_1 and CR_2 are corrosion rates (mm year^{-1}) at temperatures T_1 and T_2, E_a is the apparent activation energy for the reaction (kJ mol^{-1}), and R is the molar gas constant (8.314 J K^{-1} mol^{-1}).

The second column of Table 6 lists the values of activation energy, E_a, calculated using eqn. (10). The values of E_a obtained for systems containing varying concentrations of the investigated leaf extract are lower than in the blank solution. This finding, combined with the fact that inhibition efficiency increases with increasing temperature, suggests that the *Centrosema pubescens* leaf extract is possibly chemisorbed on the UNS S30403 surface [32].

Table 6. *Activation and thermodynamic parameters of* Centrosema pubescens *leaf extract on UNS S30403 surface in 1.0 M HCl solution*

$c_{inhibitor}$ / g L^{-1}	E_a / kJ mol^{-1}	ΔH^* / kJ mol^{-1}	$\Delta H = E_a - RT$ / kJ mol^{-1}	ΔS^* / kJ mol^{-1}	Q_{ads} / kJ mol^{-1}
0	66.69	63.47	64.17	-62.26	--
0.2	59.71	56.55	57.19	-96.09	9.13
0.4	51.64	48.55	49.12	-124.08	18.15
0.6	39.00	36.01	36.46	-166.99	31.41
0.8	26.57	23.71	24.05	-185.53	43.50
1	24.23	21.39	21.71	-219.84	44.92
1.2	20.70	17.90	18.18	-234.85	47.62
1.4	58.46	55.31	55.94	-95.97	13.39

When explaining the relationship between the temperature dependence of extract inhibition efficiency and the activation energy in the presence of the extract, it is important to remember that: (a) for extracts showing decreasing inhibition efficiency as temperature rises, the magnitude of activation energy (E_a) is higher for inhibited systems than uninhibited systems; (b) for extracts showing constant inhibition efficiency regardless of temperature, the magnitude of activation energy (E_a) does not change in the presence or absence of inhibitor; (c) for extracts with a temperature-dependent inhibition efficiency, the activation energy (E_a) in inhibited systems is lower than in extract-free media [37–42].

The observed decrease in E_a of corrosion with increasing extract concentration up to 1.2 g L^{-1} (Table 6), could be due to a shift in the net corrosion reaction from the uncovered part of the metal surface to one that directly involves adsorbed sites [40].

An alternative form of the Arrhenius equation is the transition state equation (11) [38]:

$$CR = \frac{RT}{Nh}\exp\frac{\Delta S_a^*}{R}\exp\frac{\Delta H_a^*}{RT} \quad (11)$$

where ΔS_a^* / J mol^{-1} K^{-1}- change of entropy for activation, ΔH_a^* / J mol^{-1} - change of enthalpy for activation.

According to eq. (11), the graph of ln (j_{corr}/T) *vs*. 1/*T* would give a straight line with a slope equal to $-\Delta H_a^* / R$ and intercept equal to [ln (R/Nh) + ($\Delta S_a^*/R$)]. Thus, ΔH_a^* and ΔS_a^* can be calculated from the transition-state equation. The ΔH_a^* was verified using equation (11) [32]:

$$E_a - \Delta H_a = RT \quad (12)$$

The values calculated from eq. (11) compares favorably to *RT* value, which is 2.52 kJ mol^{-1} at 303 K.

In addition to E_a, Table 6 summarizes the calculated values of ΔH_a^* and ΔS_a^*. It seems that values of E_a and ΔH_a are similar in magnitude in the extract-free medium and also when the extract is added to the medium. Both values, however, are lowering with an increase of extract leaf concentration. This finding strongly suggests that the energy barrier of the corrosion reaction was lowered in the presence of the extract without affecting the metal depletion process [41]. Furthermore, the positive sign of the activation enthalpy, ΔH_a^*, as shown in Table 6, indicates that the dissolution mechanism of UNS S30403 is endothermic in nature and slow [32,37]. In addition, the observed activation entropy, ΔS_a^*, values in the absence and presence of *Centrosema pubescens* leaf extract is negative, implying that the rate-determining step for the activated complex is the association rather than the dissociation step [6,41]. The entropy of activation, ΔS_a^*, decreased as the extract was introduced into the system (Table 6), implying that the adsorption of the extract onto the adsorbent surface was accompanied by a decrease in entropy, which is the driving force for the adsorption of the leaf extract onto the UNS S30403 austenitic stainless steel surface [42].

The heat of adsorption (Q_{ads}) of *Centrosema pubescens* leaf extract on the adsorbent surface was applied as a confirmatory test using the equation (13) [43]:

$$Q_{ads} = 2.303\left[\log\frac{\theta_2}{1-\theta_2} - \log\frac{\theta_1}{1-\theta_1}\right]\frac{T_1T_2}{T_2-T_1} \quad (13)$$

where θ_1 and θ_2 are surface coverages at two temperatures, T_1 and T_2, and R is the molar gas constant.

The last column of Table 6 shows the heat of adsorption values, Q_{ads}, which were calculated using eqn. (12) and ranged from 9.13 to 47.62 kJ mol^{-1}. These results are all positive, demonstrating that the adsorption of *Centrosema pubescens* leaf extract onto the surface of UNS S30403 austenitic stainless steel in 0.1 M HCl solution is endothermic in nature [32,41-42].

Mechanism of corrosion inhibition

Organic inhibitors are typically adsorbed on metal surfaces to control the rate of metal corrosion by disrupting either the anodic or cathodic reaction or both. The chemical structure of the inhibitor, the nature of the metal surface, the interaction between organic molecules and the metallic surface, and the type of corrosive medium influence the inhibitor adsorption process [13,16]. The leaf extract of *Centrosema pubescens* significantly controls the rate of attack of the corrosive electrolyte on the UNS S30403 austenitic stainless steel by disrupting the anodic and cathodic reactions, as shown by the potentiodynamic polarization parameters (Table 3). Because of the complex phytochemical constituents of *Centrosema pubescens* leaf extract (Table 1), it is difficult to attribute the protective effects to the adsorption of any single constituent, especially because some of these phytochemicals, such as tannins, organic and amino acids, alkaloids, proteins, flavonoids, and organic pigments, as well as their acid hydrolysis products, have been shown effective against acid corrosion of metals [22,30-32,37]. However, more research is being done to define the key active phytochemical ingredients that are responsible for the inhibitory activity of extracts. In an acid solution, for example, the hydroxyl groups in these molecules become polarized, causing the oxygen atoms to

become electron donors. As a result, hydroxyl groups may be responsible for the metal electrostatic attraction [44,45]. When these organic molecules are adsorbed onto the metal surface, they produce protective coatings with inhibitive capabilities, according to many researchers [30-31,37,40]. The extract active components could bind to the metal-aggressive solution interface in one of four ways [46-47]: (i) electrostatic interactions of protonated molecules with already adsorbed anions, and (ii) donor-acceptor interactions between π -electrons of aromatic rings and vacant d-orbitals of surface iron atoms, (iii) interaction between unshared electron pairs of hetero atoms and vacant d-orbitals of surface iron atoms, and (iv) a combination of the mechanisms described.

FTIR spectral analysis

FTIR spectra of pure *Centrosema pubescens* leaf extract and leaf extract adsorbed on UNS S30403 stainless steel surface are shown in Figure 10.

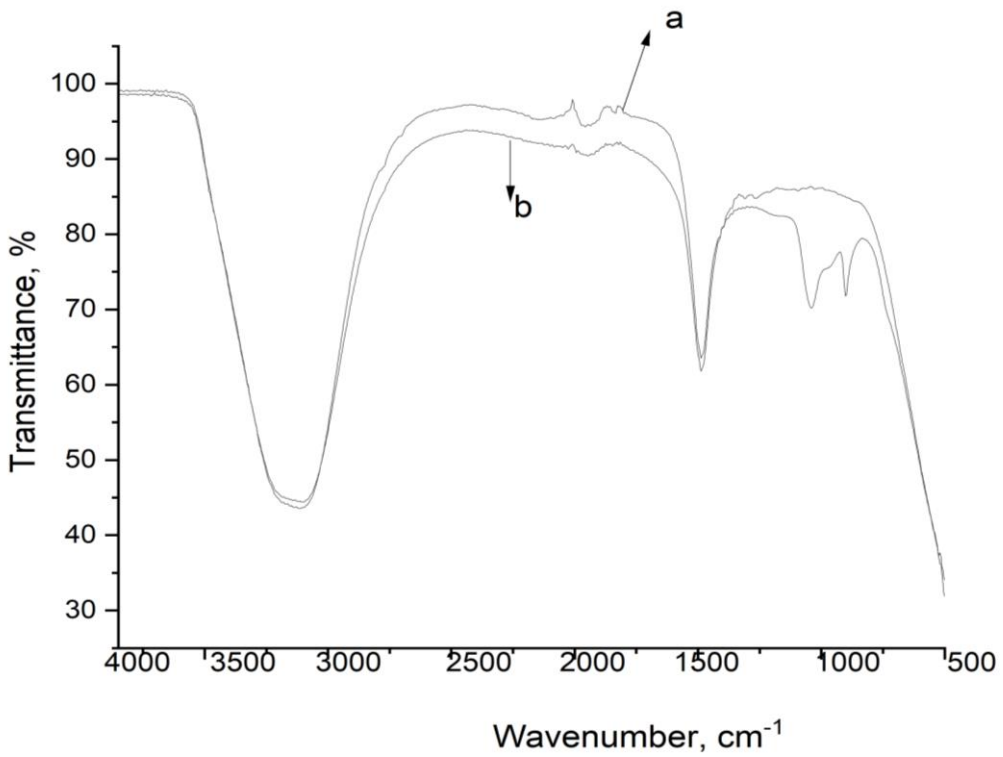

***Figure 10**. FTIR spectra of (a) pure Centrosema pubescens leaf extract and (b) surface film formed by adsorption of Centrosema pubescens leaf extract on UNS S30403*

It is obvious from Figure 10 that after adsorption on the UNS S30403 stainless steel surface, there are some changes in the FTIR spectrum of the *Centrosema pubescens* extract. The O-H peak, which appears at 3265.1 cm^{-1}, has shifted to 3250.2 cm^{-1} with reduced intensity. The C≡C peak, which appears at 2105.9 cm^{-1}, has completely disappeared. Also, the X=C=Y peak, which appears at 1982.9 cm^{-1}, has disappeared. Meanwhile, the N-H bend peak, which appears at 1636.3 cm^{-1} still remains but with reduced intensity. The peaks of C-O and C-N became visible at 1189.0 and 1051.1 cm^{-1}, respectively. The changes in the absorption pattern of these bands confirm the involvement of bonds in the adsorption of the extract components onto the stainless-steel surface. These shifts further indicate that there is an interaction between UNS S30403 austenitic stainless steel and the *Centrosema pubescens* leaf extract molecules [27,28,48].

Conclusions

Using the weight loss method, potentiodynamic polarization measurements, and morphological characterization, the corrosion inhibition effectiveness of *Centrosema pubescens* leaf extract on corrosion of UNS 30403 in 1.0M HCl solution was investigated. The main conclusions can be summarized as follows:

- The inhibition efficiency of the *Centrosema pubescens* leaf extract increases with increasing extract concentration and temperature, reaching maximum values of 93.08 and 98.66 % at 30 and 60 °C, respectively. Also, inhibition efficiency decreases with immersion time, reaching values of 86.84 and 75.00 % after 10 and 60 days at the optimal leaf extract concentration of 1.2 g L^{-1}.
- The thermodynamic investigation revealed that the leaf extract is adsorbed spontaneously on the UNS 30403 stainless steel surface, following the Langmuir adsorption isotherm model. The Gibbs free energy of adsorption (ΔG_{ads}) is found negative, indicating a significant interaction between leaf extract molecules and UNS 30403 stainless steel surface.
- According to activation, thermodynamic, and adsorption parameters, evaluated on the basis of potentiodynamic polarization measurements, the extract functions as a mixed-type inhibitor, and the adsorption of the active moieties in *Centrosema pubescens* leaf extract on the UNS S30403 surface is endothermic and occurs through mixed adsorption modes.
- The presence of a protective coating on the surface of the UNS S30403 stainless steel was confirmed by morphological and surface characterizations using SEM, EDS, XRD, and FTIR. It was found specimens in HCl solution containing optimum concentration of inhibitor extract showed less pitting corrosion occurrences, indicating that the extract of *Centrosema pubescens* leaf was able to provide enough protection.

Declaration of competing interest

The authors declare that they have no known competing financial interests or personal relationships that could have appeared to influence the work reported in this paper.

References

[1] M. Behpour, S. M. Ghoreishi, N. Soltani, M. Salavati-Niasari, *Corrosion Science* **51(5)** (2009) 1073-1082. https://doi.org/10.1016/j.corsci.2009.02.011

[2] M. Behpour, S. M. Ghoreishi, M. Khayat Kashani, N. Soltani, *Materials and Corrosion* **60** (2009) 895-898. https://doi.org/10.1002/maco.200905182

[3] A. S. Fouda, A. S. Ellithy, *Corrosion Science* **51** (2009) 868-875. https://doi.org/10.1016/j.corsci.2009.01.011

[4] H. Heydari, M. Talebian, Z. Salarvand, K. Raeissi, M. Bagheri, M. A. Golozar, *Journal of Molecular Liquids* **254** (2018) 177-187. https://doi.org/10.1016/j.molliq.2018.01.112

[5] R. Solmaz, *Corrosion Science* **79** (2014) 169-176. http://dx.doi.org/10.1016/j.corsci.2013.11.001

[6] M. Scendo, *Corrosion Science* **49(7)** (2007) 2985-3000. http://dx.doi.org/10.1016/j.corsci.2007.01.002

[7] N. Odewunmi, S. Umoren, Z. Gasem, *Journal of Environmental Chemical Engineering* **3(1)** (2015) 286-296. https://doi.org/10.1016/j.jece.2014.10.014

[8] N. I. Kairi, J. Kassim, *International Journal of Electrochemical Science* **8** (2013) 7138-7155. http://www.electrochemsci.org/papers/vol8/80507138.pdf

[9] M. Mehdipour, B. Ramezanzadeh, S. Arman, *Journal of Industrial and Engineering Chemistry* **21** (2015) 318-327. https://doi.org/10.1016/J.JIEC.2014.02.041

[10] G. M. Al-Senani, *International Journal of Electrochemical Science* **11** (2016) 291-302. http://www.electrochemsci.org/papers/vol11/110100291.pdf
[11] I. Hermoso-Diaz, J. Gonzalez-Rodriguez, J. Uruchurtu-Chavarin, *International Journal of Electrochemical Science* **11** (2016) 4253-4266. http://www.electrochemsci.org/abstracts/vol11/110604253.pdf
[12] E. Alibakhshi, M. Ramezanzadeh, G. Bahlakeh, B. Ramezanzadeh, M. Mahdavian, M. Motamedi, *Journal of Molecular Liquids* **255** (2018) 185-198. https://doi.org/10.1016/j.molliq.2018.01.144
[13] O. D. Ofuyekpone, O. G. Utu, B. O. Onyekpe, A. A. Adediran, M. Oki, *Case Studies in Chemical and Environmental Engineering* **2** (2020) 100058. https://doi.org/10.1016/j.cscee.2020.100058
[14] O. D. Ofuyekpone, O. G. Utu, B. O. Onyekpe, A. A. Adediran, *Scientific African* **11** (2021) e00714. https://doi.org/10.1016/j.sciaf.2021.e00714
[15] O. D. Ofuyekpone, O. G. Utu, B. O. Onyekpe, A. A. Adediran, M. Oki, *Chemical Data Collections* **35** (2021) 100763. https://doi.org/10.1016/j.cdc.2021.100763
[16] O. D. Ofuyekpone , O. G. Utu , B. O. Onyekpe, *Applied Surface Science Advances* **3** (2021) 100061. https://doi.org/10.1016/j.apsadv.2021.100061
[17] O. Sanni, A. P. I. Popoola, O. S. I. Fayomi, *Energy Procedia* **157** (2019) 619-625. https://doi.org/10.1016/j.egypro.2018.11.227
[18] R. T. Loto, C. A. Loto, A. P. I. Popoola, *International Journal of Electrochemical Science* **7** (2012) 7016-7032. file:///C:/Users/USER/Downloads/Effect_of_Aminobenzene_Concentrations_on_the_Corro%20(1).pdf
[19] A. K. Satpati, P. V. Ravindran, *Materials Chemistry and Physics* **109** (2008) 352-359. https://doi.org/10.1016/j.matchemphys.2007.12.002
[20] M. Lebrini, F. Robert, H. Vezin, C. Roos, *Corrosion Science* **52** (2010) 3367-3376. https://doi.org/10.1016/j.corsci.2010.06.009
[21] S. Sair, A. Oushabi, K. Nehhale, O. T. Y. Abboud, A. El Bouari, *International Journal of Electrochemical Science* **13** (2018) 10642-10653. https://doi.org/10.20964/2018.11.38 .
[22] N. Soltani, N. Tavakkoli, M. Khayatkashani, M. R. Jalali, A. Mosavizade, *Corrosion Science* **62 (1)** (2012) 122-135. https://doi.org/10.1016/j.corsci.2012.05.003
[23] K. P. Kumar, M. S. Pillai, G. R. Thusnavis, *Journal of Materials and Environmental Science* **1(2)** (2010) 119-128. https://www.jmaterenvironsci.com/Document/vol1/15-JMES-27-2010-Veno.pdf
[24] O. E. Malomo, S. A. Yaro, D. S. Yawas, A. S. Akande, *Annals of Faculty Engineering Hunedoara International Journal of Engineering* (2016). https://annals.fih.upt.ro/pdf-full/2016/ANNALS-2016-3-05.pdf
[25] V. Sribharathy, S. Rajendran, *ISRN Corrosion* **2013** (2013) 370802. http://dx.doi.org/10.1155/2013/370802
[26] M. Bouklah, B. Hammouti, *Portugaliae Electrochimica Acta* **24** (2006) 457-468. http://www.peacta.org/articles_upload/PEA_4_2006_457_468.pdf
[27] T. K. Chaitra, K. N. Mohana, H. C. Tandon, *International Journal of Corrosion* **2016** (2016) 9532809. https://doi.org/10.1155/2016/9532809
[28] G. Vengatesh, M. Sundaravadivelu, *Journal of Molecular Liquids* **287** (2019) 110906. https://doi.org/10.1016/j.molliq.2019.110906
[29] V. S. Sastri, E. Ghali, M. Elboujdaini, *Corrosion Prevention and Protection: Practical Solutions,* John Wiley & Sons Ltd, England, 2007.
[30] U.M. Eduok, M. Khaled*, Research in Chemical Intermediate* **41** (2015) 6309-6324. https://doi.org/10.1007/s11164-014-1741-3

[31] S. A. Umoren, U. M. Eduok, A. U. Israel, I. B. Obot, M. M. Solomon, *Green Chemistry Letters and Reviews* **5(3)** (2012) 303-313. https://doi.org/10.1080/17518253.2011.625980
[32] N. Soltani, N. Tavakkoli, M. Khayat Kashani, A. Mosavizadeh, E. E. Oguzie, M. R. Jalali, *Journal of Industrial and Engineering Chemistry* **20(5)** (2014) 3217-3227. https://doi.org/10.1016/j.jiec.2013.12.002
[33] S. Deng, X. Li, *Corrosion Science* **64** (2012) 253-262. https://doi.org/10.1016/j.corsci.2012.07.017
[34] X. Li, S. Deng, H. Fu, *Corrosion Science* **62** (2012) 163-175. https://doi.org/10.1016/j.corsci.2012.05.008
[35] R. Jenkins, R.L. Snyder, *Introduction to X-ray Powder Diffractometry*, John Willey & Sons Inc., New York, 1996. http://dx.doi.org/10.1002/9781118520994
[36] A. Hamdy, Nour Sh. El-Gendy, *Egyptian Journal of Petroleum* **22** (2013) 17-25. http://dx.doi.org/10.1016/j.ejpe.2012.06.002
[37] I. Dehri, M. Özcan, *Materials Chemistry and Physics* **98(2-3)** (2006) 316-323. https://doi.org/10.1016/j.matchemphys.2005.09.020
[38] T. Szauer, A. Brandt, *Electrochimica Acta* **26(9)** (1981) 1209-1217. https://doi.org/10.1016/0013-4686(81)85107-9
[39] I. B. Obot, N. O. Obi-Egbedi, S. A. Umoren, *Corrosion Science* **51** (2009) 1868-1875. http://dx.doi.org/10.1016/j.corsci.2009.05.017
[40] O. L. Riggs Jr, R. M. Hurd, *Corrosion* **23(8)** (1967) 252-260. http://dx.doi.org/10.5006/0010-9312-23.8.252
[41] M. Scendo, *International Journal of Electrochemical Science* **8** (2013) 9201-9221. http://www.electrochemsci.org/papers/vol8/80709201.pdf
[42] J. I. Bhat, V. D. P. Alva, *International Journal of Electrochemistry* **2011** (2011) 157576. http://dx.doi.org/10.4061/2011/157576
[43] O. E. Nnabuk, A. Femi, E. E. Ebenso, *International Journal of Electrochemical Science* **5** (2010) 1996-2011. http://www.electrochemsci.org/papers/vol5/5121996.pdf
[44] O. Sanni, A. P. I. Popoola, O. S. I. Fayomi, *Journal of Bio- and Tribo-Corrosion* **5** (2019) 88. https://doi.org/10.1007/s40735-019-0280-2
[45] R. T. Loto, C. A. Loto, A. P. I. Popoola, T. Fedotova, *Arabian Journal of Chemistry* **12(8)** (2015) 2270-2279. https://doi.org/10.1016/j.arabjc.2014.12.024
[46] C. O. Akalezi, C. E. Ogukwe, E. A. Ejele, E. E. Oguzie, *Interntional Journal of Corrosion and Scale Inhibition* **5(3)** (2016) 232-247. https://doi.org/10.17675/2305-6894-2016-5-3-4
[47] R. T. Loto, C. A. Loto, *International Journal of Electrochemical Science* **7** (2012) 9423-9440. http://www.electrochemsci.org/papers/vol7/71009423.pdf
[48] A. S. Fouda, S. M. Rashwan, M. Abdelfatah, *Zaštita Materijala* **60(1)** (2019) 3-17. http://dx.doi.org/10.5937/zasmat1901003F